Sensitivity analysis of a nanowire-based surface plasmon resonance biosensor in the presence of surface roughness

Kyung Min Byun

School of Electrical Engineering and Computer Science, Seoul National University, Seoul, Korea 151-742

Soon Joon Yoon and Donghyun Kim

School of Electrical and Electronic Engineering, Yonsei University, Seoul, Korea 120-749

Sung June Kim

Nano Bioelectronics and Systems Research Center, Seoul National University, Seoul, Korea 151-742

Received July 14, 2006; accepted August 16, 2006;
posted September 5, 2006 (Doc. ID 73039); published January 10, 2007

We have investigated the effect of surface roughness on the sensitivity of conventional and nanowire-based surface plasmon resonance (SPR) biosensors. The theoretical research was conducted using rigorous coupled-wave analysis with Gaussian surface profiles of gold films determined by atomic force microscopy. The results suggest that, when surface roughness ranges near 1 nm, the sensitivity of a conventional SPR system is not significantly affected regardless of the correlation length. For a nanowire-based SPR biosensor, however, we have found that the sensitivity degrades substantially with decreasing correlation length. In particular, at a correlation length smaller than 100 nm, a random rough surface may induce destructive coupling between excited localized surface plasmons, which can lead to prominent reduction of sensitivity enhancement.

OCIS codes: 050.2770, 130.6010, 240.0310, 240.6680.

1. INTRODUCTION

When TM-polarized light is incident on a dielectric–metal interface, a collective motion of electrons, surface plasmons (SPs), is created at a specific incidence angle, which is known as surface plasmon resonance[1] (SPR). The excitation of SPs, as a result of the momentum matching between incident photons and SPs, is accompanied by radiative and thermal damping of the incident light energy, whereby the light intensity reflected from a thin metal film becomes minimal. A small change in refractive indices of the environment surrounding the metal surface induces a shift of the SPR condition. By measuring the resonance shift, one can monitor biological and chemical interactions on a quantitative basis in real time. Since the introduction of Kretschmann's configuration in 1972,[2] SPR-based biosensors have been widely used as optical biosensors to detect and analyze various biochemical reactions.[3–6]

In recent years, localized surface plasmons (LSPs) have drawn tremendous interest for SPR signal amplification.[7] As metallic nanostructures are illuminated, incident photons are coupled into SP modes localized in the nanostructures. LSPs typically involve a large number of modes, and momentum matching usually is achieved at higher momentum than bulk SP modes. Excited LSP modes can induce resonant field enhancements through strong absorption and highly efficient light scattering. Such enhancement of local electromagnetic fields is mainly dependent on the size, shape, and distribution of the nanostructures. Modified SPR biosensing systems that consist of noninteracting or interacting metallic nanostructures have been proposed for various sensing applications.[8–11] Experimental results show that LSP resonance (LSPR) biosensors amplify the detected shift of resonance angle or wavelength and thus lead to an improvement of sensitivity by more than ten times compared with a conventional SPR biosensor without metallic nanostructures.

In previous studies, we investigated the effects of gold nanowires numerically to design a SPR biosensor with extremely high sensitivity using regularly patterned one-dimensional nanowires.[12–15] Despite fundamental restraints imposed by surface plasmon polariton (SPP)–LSP interactions, resonantly excited LSP modes from gold nanowires and optical coupling between the LSP modes can dramatically increase local resonant fields. The results showed that local-field enhancement significantly affects the sensor performance and has positive correlation with the sensitivity. An assumption inherent in these studies is that the surface of thin films and nanowires is perfectly flat. In practice, however, surface roughness always exists on a substrate and thin films, which may affect the properties of the excited LSP modes substantially.

The impact of rough surfaces on SPR characteristics has been extensively investigated in Ref. 1, where Raether considered the surface roughness rather thoroughly in two regimes. When the surface is of small roughness in the range of 0.5–2 nm, nonradiative SPs become radiative as a result of the optical coupling between excited SPs and photons. In addition, a strong electromagnetic field takes place in the metal surface when it is not localized. On the other hand, for roughness larger than 5 nm, excited plasmons are strongly scattered and move with increased disorder, less like a propagating wave. Especially, for very rough surfaces, a significant change in the dispersion relation is observed as the accumulation of electromagnetic fields results in highly enhanced and localized plasmons. Michel *et al.* also studied the influence of rough corrugation on SPR responses, and they revealed the scattering properties due to the excitation of SPs on a randomly rough surface involving a periodic component.[16]

In this work, we focus on the effect of roughness on the sensitivity of a nanowire-based SPR sensor. Since the size of metallic nanostructures introduced to excite LSPs is generally in the range of a few tens of nanometers, the resonant field enhancement can be substantially influenced by small changes in a surface profile. As a result, SPR biosensors with nanowires may suffer from degraded sensitivity. More specifically, we investigate the impact of the surface fluctuation on the sensitivity of a LSPR-based biosensor by modeling metallic nanowires on a rough surface as the sum of periodic rectangular gratings and one-dimensional Gaussian random surfaces. The random surface with Gaussian statistics is a fundamental model with two independent parameters: the surface roughness (δ), which for clarification is quantitatively defined as the root-mean-square (rms) surface height deviation from a mean plane, and the correlation length (CL) of the surface profile. In this study, these parameters have been determined experimentally by atomic force microscopy (AFM) measurements of thin gold films deposited on a generic glass substrate.

Furthermore, we explore and compare two cases: (i) a gold surface with flat or Gaussian random profiles for a conventional SPR system and (ii) periodic gold nanowires superposed on a flat or random Gaussian gold surface for a nanowire-mediated SPR system. Here, a flat surface indicates a thin gold film with no Gaussian random component and bears no relation to the existence of nanowire arrays. In other words, flat nanowires indicate that the tops and valleys of nanowires do not take statistical profiles. To measure the effect of the surface fluctuation on the sensitivity, we define target analytes as a self-assembled monolayer (SAM), which covers both gold nanowires and a gold film. Although the study is conducted on a SPR sensor structure that employs one-dimensional nanowires to excite LSPs, the results can be equally valid to interpret more complicated nanostructures.

The presentation is organized as follows. In Section 2, random Gaussian rough surfaces of interest and a model based on rigorous coupled-wave analysis (RCWA) are described. Numerical results on the sensitivity of nanowire-based SPR biosensors with random surfaces are presented and discussed in comparison with a conventional SPR structure in Section 3, which is followed by concluding remarks in Section 4.

2. NUMERICAL METHODS

To extract parameters of a typical surface employed in a SPR biosensor, we have measured surface profiles of a thin gold film deposited on a slide glass using an atomic force microscope (PSIA, XE-150, contact mode). A 40 nm thick gold film was thermally evaporated under pressure of 4×10^{-6} Torr on a BK7 glass substrate after a 2 nm chrome layer was applied to increase the adhesion of gold to the slide glass. The glass substrate is a generic slide glass (Marienfeld GmbH, Germany). Three of the fabricated samples have been prepared for AFM measurements. AFM images have been acquired with a scanning length of 5 μm. The probability density function of surface height data measured of a sample and its autocorreation function are shown in Fig. 1. The height distribution and its Gaussian fit are well matched for all three samples, and thus they successfully approximate Gaussian random surfaces to the first degree. Table 1 summarizes the measured rms roughness values and $1/e$ CLs for

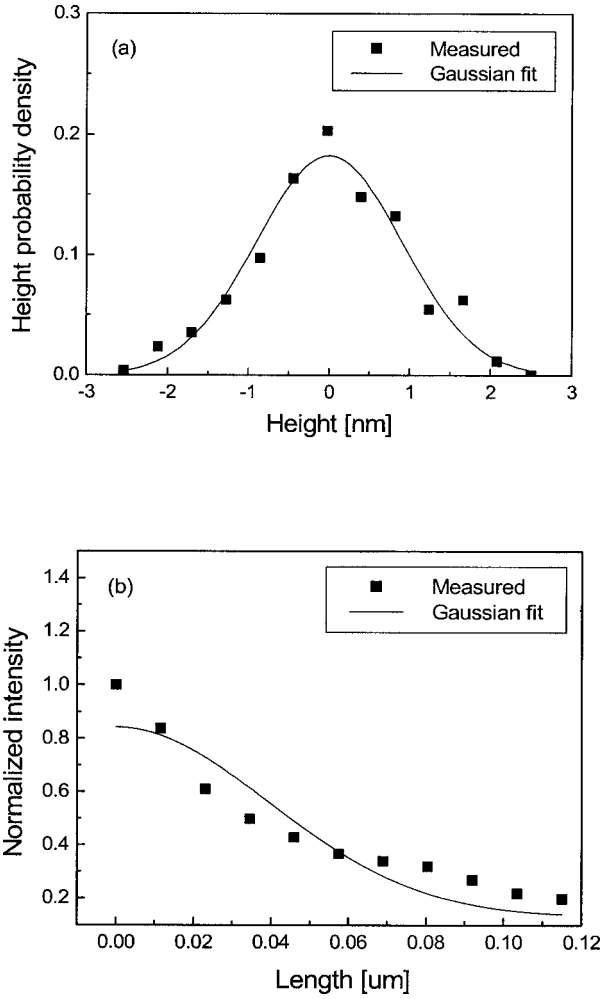

Fig. 1. (a) Measured height probability density of sample C (squares) using the AFM. The solid curve is its optimal Gaussian fit. (b) Numerical distribution of the height correlation of sample C (squares) and its Gaussian fit (solid curve).

Table 1. Experimentally Measured rms Roughness Values and CLs for Three Samples (A, B, C) of Thin Gold Films on Glass Substrates

Measurement	Sample A	Sample B	Sample C
Rms roughness, δ (nm)	1.16	0.75	0.97
Correlation length, CL (nm)	150	100	60

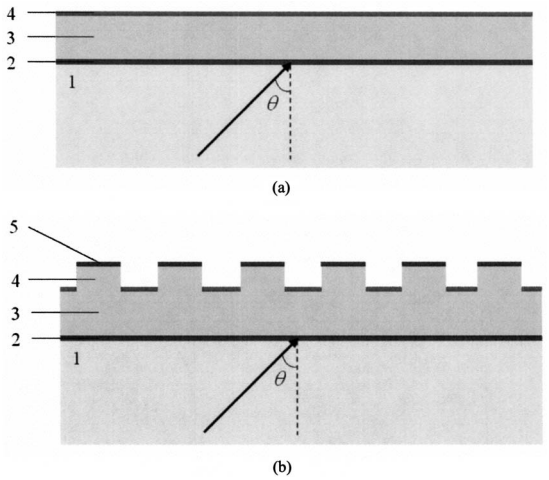

Fig. 2. (a) Schematic diagram of a conventional SPR biosensor. A TM-polarized light with a wavelength $\lambda=633$ nm is incident at an angle θ. Layers 1, 2, 3, and 4 indicate a BK7 glass substrate, an attachment layer of chrome, a thin gold film, and target analytes, respectively, in air environment. The thicknesses of the layers are 2 nm (d_2), 40 nm (d_3), and 3 nm (d_4). (b) Schematic diagram of a nanowire-based SPR biosensor with periodic gold nanowires on a gold film. Compared with a conventional SPR configuration in (a), the structures are identical except for an additional layer of 20 nm thick nanowire arrays.

the three samples. Note that the CLs of the random surfaces exhibit notable deviations from a few tens of nanometers to more than 100 nm in dimension. This discrepancy of the CLs is presumably associated with the surface condition of glass substrates as well as the specific metal deposition process. Based on, Table 1, a range of values have been considered for the CL in modeling random Gaussian surfaces.

Figure 2 presents schematic diagrams of a conventional and a nanowire-based SPR biosensor with rectangular gold nanowires. The surface profiles in Fig. 2 were subsequently modulated by Gaussian random statistics with four different random surface profiles, shown in Fig. 3, and used in our calculation for a conventional SPR system. The Gaussian random surface is characterized with $\delta=1$ nm and CL=50, 100, 200, and 500 nm. The overall surface dimension under consideration is set to be 5 μm. An additional layer of binding analytes coated on a randomly corrugated gold surface has been modeled as a 3 nm thick SAM with refractive index $n_{\mathrm{SAM}}=1.52643$ and is assumed to replicate the gold surface profile under the SAM. Note that it is statistically more relevant to average the performance of many realizations of rough surfaces for a given CL. However, for short CLs less than 100 nm, the overall surface dimension of 5 μm is much larger than the CLs, so that a significant number of variations are included in the constructed surface profiles, which can result in average SPR characteristics for the random rough surfaces. On the other hand, a surface with longer CLs obviously approaches the flat surface. This indicates that the use of a single rough surface, if its overall surface dimension is sufficiently large compared with CLs, can provide valid insights on the average roughness performance.

Similarly, nanowire arrays modeled with random rough surfaces are shown in Fig. 4. The solid and dotted curves represent rectangular nanowire gratings deposited on the gold film with a Gaussian random statistic and 3 nm thick binding analytes, respectively. The binding layer covers both surfaces of the thin film and nanowires. At each CL, the surface profile of the thin-film baseline is assumed to be identical to that of Fig. 3. The nanowire depth and the period (Λ) are fixed at 20 and 200 nm, respectively, with a fill factor $f=0.5$.

Once the surface profiles are designed, RCWA has been used to calculate the sensitivity of SPR biosensors and to study the impact of the surface fluctuation on the sensitivity enhancement in a nanowire-based SPR biosensor.[17,18] RCWA has been successfully applied to obtaining optical characteristics of various nanostructures and explaining the measurements that involve nanostructures.[19–22] As illustrated in Fig. 2, TM-polarized illumination with $\lambda=633$ nm is assumed to be incident on a metal–dielectric interface at an angle θ. The dielectric functions (n,k) of a glass substrate, chrome, and gold are, respectively, given as (1.515, 0), (3.48, 4.36), and (0.18, 3.0) at $\lambda=633$ nm.[23]

3. RESULTS AND DISCUSSION

To evaluate the performance on a quantitative basis, a sensitivity enhancement factor (SEF) has been defined as

$$\mathrm{SEF}=\Delta\theta_{\mathrm{SPR}}/\Delta\theta_{\mathrm{SPR\_REF}}, \tag{1}$$

where $\Delta\theta_{\mathrm{SPR\_REF}}$ represents the plasmon resonance angle difference induced by the presence of binding analytes for a flat gold surface without nanowires. $\Delta\theta_{\mathrm{SPR}}$ is the resonance angle difference calculated for the surface under test, for instance, a flat surface without nanowires or a rough, i.e., Gaussian random, surface for conventional or nanowire-based SPR structures.

The SEF has been calculated for the surface profiles of gold films modulated by random rough surfaces at four different CLs. First, we consider the influence of the Gaussian random surface on the sensitivity of a conventional SPR configuration, as shown in Fig. 2(a). Figure 5 presents the calculated reflectance as a function of incidence angle for a flat and a Gaussian random surface. For the ideal flat surface, resonance angles with and without binding analytes are, respectively, 45.65° and 45.13°: thus the resonance shift ($\Delta\theta_{\mathrm{SPR\_REF}}$) in Eq. (1) is 0.52°. When the gold film takes a Gaussian profile at CL=50 nm, the SPR angles increase to 45.90° with analytes and 45.35° without analytes: the shift then is 0.55°. Table 2 summarizes SPR characteristics of Gaussian surfaces with varying CLs that range from 50 to 500 nm. It shows that resonance angles (θ_{SPR}) as well as the resonance angle shift ($\Delta\theta_{\mathrm{SPR}}$) demonstrate a minor increment as CL decreases.

It is interesting to note that, for CL$<$200 nm, the sensitivity of a rough surface with a Gaussian random profile becomes slightly larger than that of a flat gold surface. While it is easy to presume hastily that the introduction of roughness may enhance the sensitivity for any Gaussian surface with a small CL, it is also necessary to consider the results in Table 2 in terms of the deviation range. For example, when the overall surface length is 5 μm and CL=50 nm, the deviation range, which can be estimated to be proportional to $N^{-1/2}$ with N as the ratio of the surface length to CL, is equal to 10%. Since the calculated increase of the SEF by 6% at CL=50 nm falls in this range, the sensitivity increase may result from a particular Gaussian surface, and it is thus difficult to conclude that an increment of sensitivity is expected for an arbitrary Gaussian surface profile of a small CL.

By comparison, it has been observed that the performance of a conventional SPR structure is affected very little when the film roughness δ is as small as 1 nm. In this case, the effect of surface fluctuation on the sensitivity is practically limited and insignificant irrespective of the CL, since the excited SPs propagating along the metal surface are still dominant and there is less interference from rough surfaces.

Second, we are interested in the impact of roughness on a nanowire-based SPR configuration in terms of sensitivity as CLs of a Gaussian random surface are varied. In a nanowire-based SPR biosensor, shown in Fig. 2(b), one-dimensional rectangular nanowires are used to induce excitation of LSP modes. Compared with a conventional SPR structure of Fig. 2(a), the presence of nanostructures near the metal surface creates a large disturbance of the dispersion relation of SPP modes. In particular, when the LSP resonance condition is satisfied, propagating SPP modes are highly damped while the local fields are considerably enhanced, which consequently leads to improved sensitivity. This well-known performance of LSP modes can be confirmed in Fig. 6. Gold nanowire arrays fabricated on a flat gold surface with Λ=200 nm and f=0.5 shift the resonance angle θ_{SPR} by 0.95°, which results in SEF=1.83. As will be described later, this SEF value can be further improved as the nanowire period decreases to smaller than 200 nm.

The existence of surface roughness may deteriorate the sensitivity of a nanowire-based SPR biosensor. For the Gaussian random surface with CL=50 nm, $\Delta\theta_{SPR}$=0.57°, i.e., SEF=1.10. The reflectance characteristics of the structure are also shown in Fig. 6. Table 3 lists the calcu-

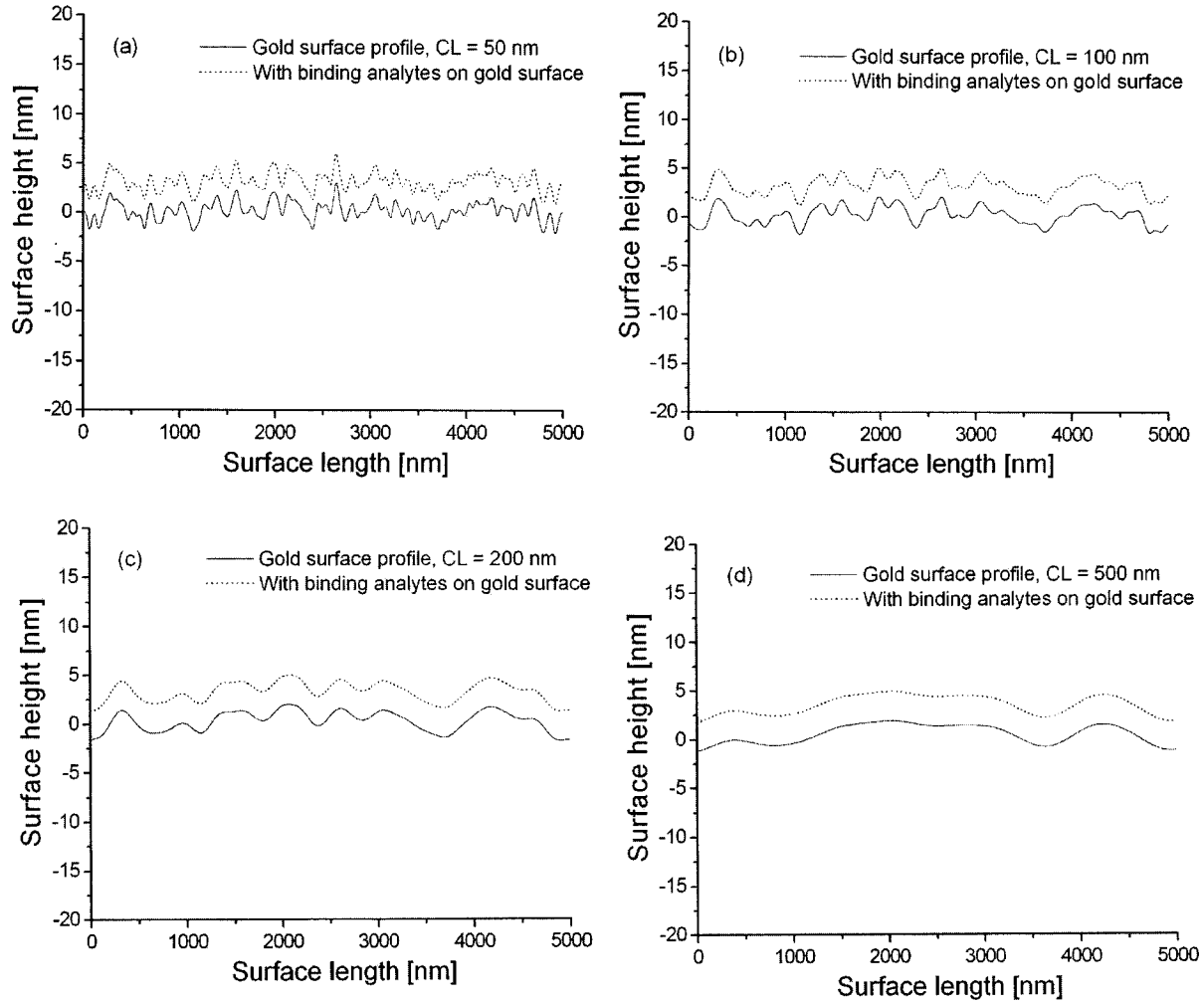

Fig. 3. Gaussian random profiles of a gold surface used in the calculation for a conventional SPR configuration. The overall surface length is 5 μm, and the surface roughness δ=1 nm. The solid and dotted curves represent the surface profiles of a thin gold film and 3 nm thick binding analytes on a gold film. The CLs are (a) 50, (b) 100, (c) 200, and (d) 500 nm.

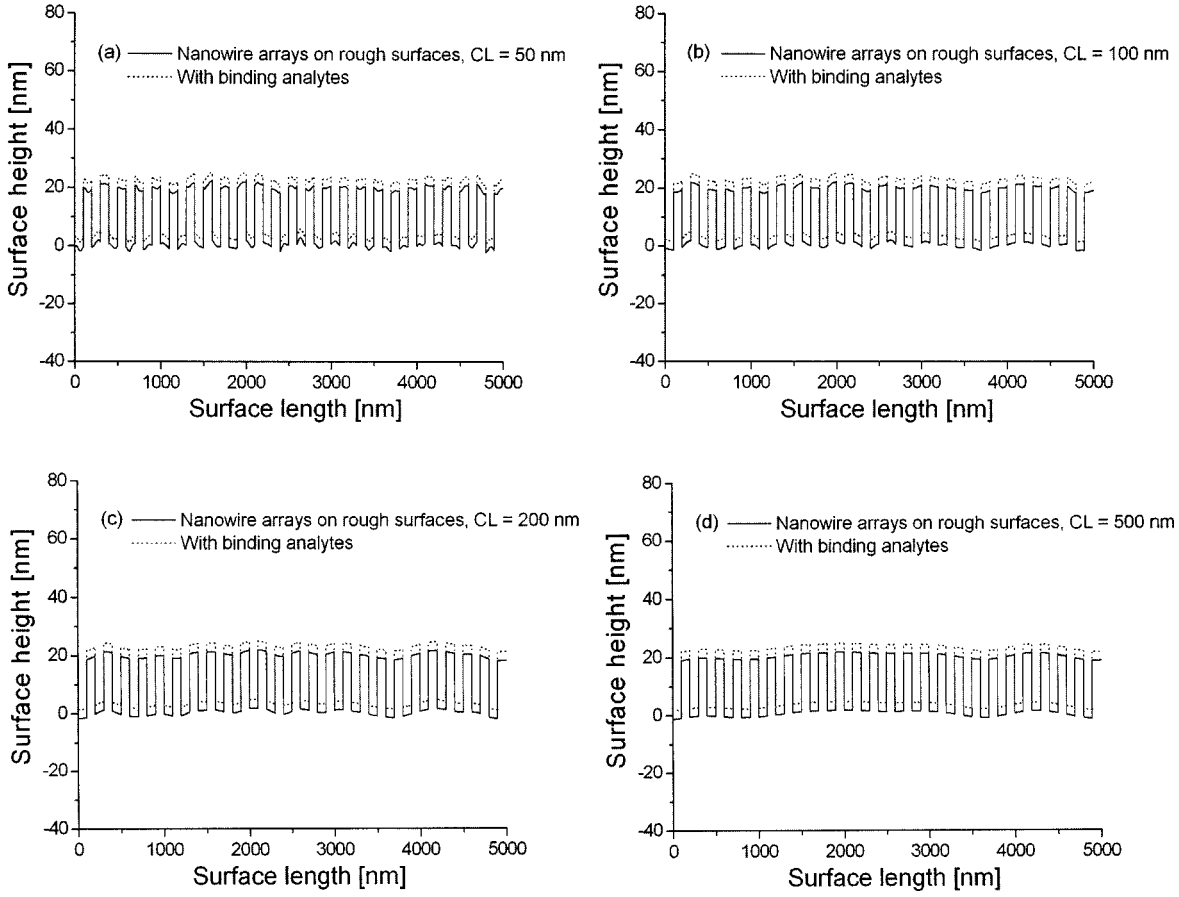

Fig. 4. Surface profiles of a gold film involving periodic nanowires. For a nanowire-based SPR configuration, the surface profile is modeled as a sum of rectangular gratings and Gaussian random surfaces. The nanowire arrays with a fill factor $f=0.5$ and $\Lambda=200$ nm are 20 nm thick. The overall surface length is 5 μm, and the surface roughness $\delta=1$ nm. The solid and dotted curves represent the surface profiles of a gold film involving nanowires and 3 nm thick binding analytes. The CLs are (a) 50, (b) 100, (c) 200, and (d) 500 nm. For each CL, the Gaussian random profile is assumed to be identical to that of Fig. 3.

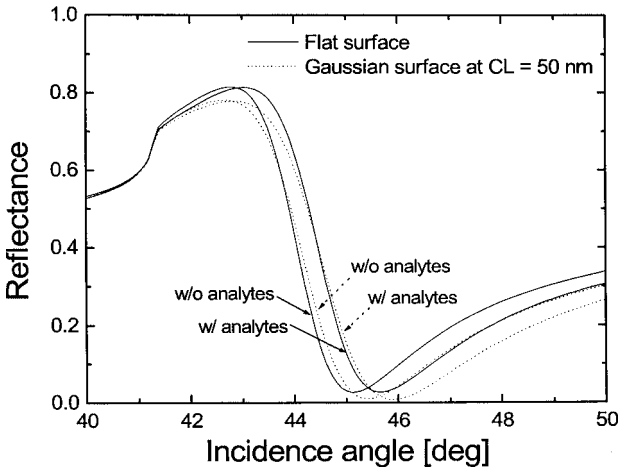

Fig. 5. Calculated reflectance curves for perfectly flat and rough surfaces in a conventional SPR biosensor shown in Fig. 2(a). The solid curves are for a flat surface with the resonance angles 45.65° (with binding analytes) and 45.13° (without binding analytes). The dotted curves are for a Gaussian random surface with $\delta=1$ nm and CL=50 nm. The resonance angles with and without binding analytes are 45.90° and 45.35°, respectively.

lation results regarding the sensitivity enhancement at different CLs. The SEF is reduced in general with a decreasing CL. For CL$<$100 nm, SEF drops significantly, which far exceeds the deviation range and thus validly demonstrates that the excitation of LSP modes induced by periodic nanowires is disrupted by the Gaussian rough surface.

Table 2. Calculation Results of SPR Characteristics of Gaussian Random Surfaces for a Conventional SPR Configuration

	Correlation Length (nm)			
Characteristic	50	100	200	500
θ_{SPR} (w/o analytes) (deg)	45.35	45.17	45.16	45.15
θ_{SPR} (w/ analytes) (deg)	45.90	45.71	45.68	45.63
$\Delta\theta_{SPR}$ (deg)	0.55	0.54	0.52	0.48
SEF	1.06	1.04	1.00	0.92

To effectively investigate the influence of the rough surface on the sensitivity, we have considered nanowire arrays with a period shorter than 200 nm (see Fig. 7). Generally, with a shorter nanowire period, near-field interactions between neighboring nanowires encourage electromagnetic coupling that is responsible for intensely enhanced local fields. Figure 7 upholds that SEF values for flat nanowire arrays are notably improved by reducing

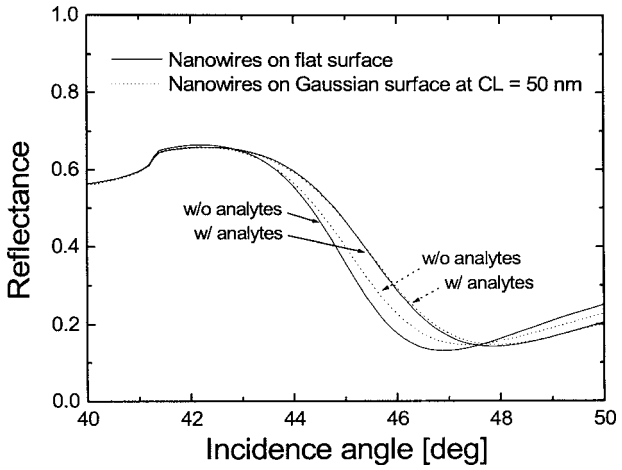

Fig. 6. Calculated reflectance curves for perfectly flat and rough surface's in a nanowire-based SPR biosensor shown in Fig. 2(b). The solid curves are for nanowires on a flat surface (flat nanowires) with resonance angles of 46.90° (with binding analytes) and 47.85° (without binding analytes). The dotted curves are for nanowires on a Gaussian random surface with $\delta=1$ nm and CL $=50$ nm. The resonance angles with and without binding analytes are 47.36° and 47.93°, respectively.

Table 3. Calculation Results of SPR Characteristics of Gaussian Random Surfaces for a Nanowire-based SPR Configuration[a]

	Correlation Length (nm)			
Characteristic	50	100	200	500
θ_{SPR} (w/o analytes) (deg)	47.36	47.10	47.07	46.91
θ_{SPR} (w/ analytes) (deg)	47.93	47.88	47.95	47.85
$\Delta\theta_{SPR}$ (deg)	0.57	0.78	0.88	0.94
SEF	1.10	1.50	1.69	1.81

[a]Nanowire period and depth are 200 and 20 nm

nanowire periods. Figure 7 also suggests that the sensitivity, if CL is fixed, becomes enhanced with shorter nanowire periods for a LSP-based sensor that employs rough nanowires. From the results, it is confirmed that the significant improvement of sensitivity by the excited LSP modes is a typical characteristic for a SPR biosensor involving nanostructures.[12,13]

With a decrease in the CL, we observe less enhanced sensitivity compared with flat nanowires (the dotted lines in Fig. 7), which in effect is equivalent to a rough surface with an infinite CL. When the CL approaches zero, the correlation present in the surface profile disappears more quickly, and a completely random profile emerges within given surface randomness. As an aperiodic component of the surface becomes prominent, it suppresses excited LSP modes due to the interference between highly random surfaces and periodic nanowire arrays. Numerical results in the case of $\Lambda=80$ nm find that the SEF values for CL $=20$ and 200 nm are 2.31 and 3.20, respectively. This suggests that sensitivity degradation larger than 30% may be introduced by extremely rough surfaces.

Maradudin and co-workers present the effects of surface roughness on the dispersion relation of the propagating SPs.[24,25] They proved the splitting of the SP dispersion curve was caused by surface roughness. In the presence of roughness, the frequency of SPPs was obtained as

$$w_{\pm}(\xi) = w_0 \pm \frac{2\sqrt{2}}{\varepsilon'(w_0)}\frac{\delta}{\alpha}\frac{f(\xi)}{\left[1+\frac{1}{2}(\delta/\alpha)^2\xi^2\right]^{1/2}}, \quad (2)$$

where w_0 is the resonance frequency of me SPs on a flat surface. δ and α are the rms surface roughness and the CL, respectively. ξ is the dimensionless wave vector ($=k\alpha$, where k is the magnitude of the wave vector), and $f(\xi)$ is an infinite series as a function of ξ. From Eq. (2), the second term indicates the perturbative roughness-induced frequency shift and is largely proportional to the ratio (δ/α) with minor dependence on $(\delta/\alpha)^2$. The splitting of the SP dispersion curve vanishes as ξ approaches zero or infinity. In either case, SP is associated with a flat surface. Thus, its resonant frequency is equal to that of a flat surface (w_0).

We also confirm that qualitative trends inferred from the above expression agree decently with our numerical results for a range of the parameters that we use to characterize the surface profile. When $\delta=1$ nm and the CL (α) ranges from 50 to 500 nm, comparable with SP wavelength, the ratio (δ/α) is quite small, and the resonant frequency variation also becomes limited. Thus, at a relatively large CL in Table 2, the resonance angle is close to that of a flat surface. With a decrease of CL, the deviation of frequency shift is larger, and the resonance angle θ_{SPR} as well as its shift $\Delta\theta_{SPR}$ generally increases, as presented in Table 2. With reference to the explicit expressions of Eq. (2), it is expected that if $\delta \gg 1$ nm, the effect of surface roughness on the sensitivity of a conventional SPR system would be more pronounced.

In the case of a nanowire-based SPR system, the existence of nanowires on a metal surface may lead to considerable deformation of the dispersion relation of SPPs as described earlier. When localized plasmons confined to metallic nanowires are dominantly excited, the propagating SPs are extremely damped, and the local-field en-

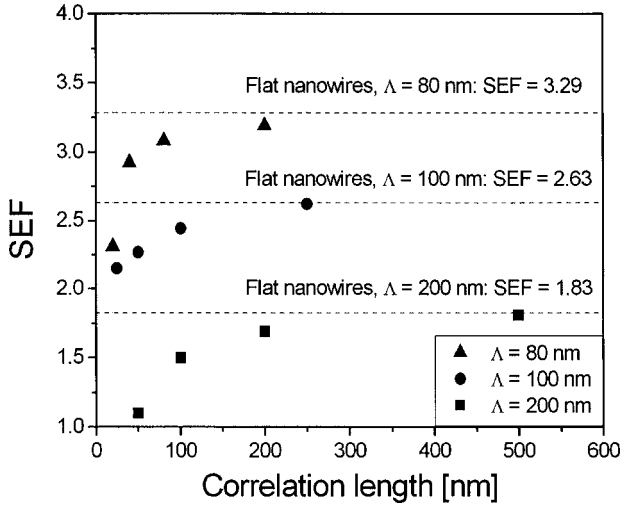

Fig. 7. SEF characteristics with a varying CL at $\Lambda=80$ nm (triangles), 100 nm (circles), and 200 nm (squares). The dotted lines present the SEF values of flat nanowires for a given nanowire period.

hancement induces amplification of SPR signals. In particular, for interacting nanowires, if $\Lambda \ll \lambda$, electromagnetic coupling between nanowires has prominent impact on the resonance condition. With a considerably short period, short-range interactions incur near-field coupling that creates highly sensitive plasmons confined to metal boundaries and leads to additional resonance.[26,27] However, when there is a rough surface with a short CL comparable with the nanowire dimension, SEF drops abruptly owing to the destructive coupling mechanism between nanowires as LSPs are driven out of phase and result in disordered interactions.[28] If $\delta > 1$ nm, although it is not considered here in detail, the disturbance effect of the random surface on the coupling of local fields becomes more prominent, which gives rise to additional degradation of the resonance modes.

In terms of actual implementation of a LSPR-based biosensor, the use of nanowires regularly patterned on a thin metal film yields a structure that can provide highly improved efficiency with reproducible performance. This study suggests the need for considering the surface parameters of a metal film and their effects on the sensitivity, since the sensitivity that can be achieved in a nanowire-based SPR biosensor can be compromised depending on the surface quality.

4. CONCLUSION

In this paper, we have considered the effect of surface roughness on the sensitivity of a SPR biosensor. Our calculation results showed that for a conventional SPR configuration the surface roughness has a limited influence on the sensitivity enhancement regardless of the CL. Although a trivial increment of sensitivity is observed with a decreasing CL, it appears insignificant to justify the sensitivity increase for an arbitrary Gaussian rough surface. Moreover, the disturbance of the dispersion relation and resonance condition is negligible, since the roughness of 1 nm is sufficiently small and thus the excitation of propagating SPs is still dominant. However, when surface roughness increases significantly, possibly due to the imperfection of the fabrication process, very rough surfaces can induce notable deformation in the dispersion relation and highly enhanced localized plasmons, which results in great discrepancy between expected and actual SEF characteristics of a conventional SPR system.

We have also investigated a nanowire-based SPR configuration in which LSPs are mainly at work to improve the sensitivity. In contrast to a conventional scheme, surface roughness as small as 1 nm showed a substantial effect on the sensitivity while its enhancement deteriorated by more than 30% at a short CL < 100 nm. As the excited localized plasmons on a fiat surface are interacting positively with neighbors in short distances, the presence of surface fluctuation causes disordered coupling between nanowires and consequently discourages the enhancement of the sensitivity. It has been confirmed that the influence of the destructive interactions on the sensitivity degradation was substantial for nanowires with $\Lambda < 200$ nm. From this study, it is highly recommended that the surface roughness be taken into consideration when designing and fabricating a SPR biosensor for desired sensitivity performance.

ACKNOWLEDGMENTS

This work was supported by the Korea Science and Engineering Foundation (KOSEF) through the National Core Research Center for Nanomedical Technology (R15-2004-024-00000-0) and also by the Korea Research Foundation (KRF) grant funded by the Korean Government, the Ministry of Education and Human Resources Development (MOEHRD), under KRF-2005-205-D00051. K. M. Byun and S. J. Kim acknowledge support by the Engineering Research Center (ERC) program of the Ministry of Science and Technology (MOST)/KOSEF (R11-2000-075-01001-1). We appreciate Hyun Seok Lee and Professor Kyung Hwa Yoo for kindly providing assistance for the AFM measurements.

Corresponding author D. Kim can be reached by e-mail at kimd@yonsei.ac.kr.

REFERENCES

1. H. Raether, *Surface Plasmon on Smooth and Rough Surfaces and on Gratings* (Springer-Verlag, 1988).
2. E. Kretschmann, "Decay of non radiative surface plasmons into light on rough silver films: comparison of experimental and theoretical results," Opt. Commun. **6**, 185–187 (1972).
3. M. Malmqvist, "Surface plasmon resonance for detection and measurements of antibody–antigen affinity and kinetics," Curr. Opin. Immunol. **5**, 282–286 (1993).
4. B. P. Nelson, T. E. Grimsrud, M. R. Liles, R. M. Goodman, and R. M. Corn, "Surface plasmon resonance imaging measurements of DNA and RNA hybridization adsorption onto DNA microarrays," Anal. Chem. **73**, 1–7 (2001).
5. R. J. Leatherbarrow and P. R. Edwards, "Analysis of molecular recognition using optical biosensors," Curr. Opin. Chem. Biol. **3**, 544–547 (1999).
6. B. Liedberg, C. Nylander, and I. Lundstrom, "Biosensing with surface plasmon resonance—how it all started," Biosens. Bioelectron. **10**, 1–4 (1995).
7. E. Hutter and J. H. Fendler, "Exploitation of localized surface plasmon resonance," Adv. Mater. (Weinheim) **16**, 1685–1706 (2004).
8. L. A. Lyon, D. J. Pena, and M. J. Natan, "Surface plasmon resonance of Au colloid-modified Au films: particle size dependence," J. Phys. Chem. B **103**, 5826–5831 (1999).
9. L. He, M. D. Musick, S. R. Nicewarner, F. G. Salinas, S. J. Benkovic, M. J. Natan, and C. D. Keating, "Colloidal Au-enhanced surface plasmon resonance for ultrasensitive detection of DNA hybridization," J. Am. Chem. Soc. **122**, 9071–9077 (2000).
10. A. D. McFarland and R. P. Van Duyne, "Single silver nanoparticles as real-time optical sensors with zeptomole sensitivity," Int. Chem. Eng. **3**, 1057–1062 (2003).
11. A. J. Haes and R. P. Van Duyne, "A nanoscale optical biosensor: sensitivity and selectivity of an approach based on the localized surface plasmon resonance spectroscopy of triangular silver nanoparticles," J. Am. Chem. Soc. **124**, 10596–10604 (2002).
12. K. M. Byun, S. J. Kim, and D. Kim, "Design study of highly sensitive nanowire-enhanced surface plasmon resonance biosensors using rigorous coupled wave analysis," Opt. Express **13**, 3737–3742 (2005).
13. K. M. Byun, D. Kim, and S. J. Kim, "Investigation of the profile effect on the sensitivity enhancement of nanowire-mediated localized surface plasmon resonance biosensors," Sens. Actuators B **117**, 401–407 (2006).
14. K. M. Byun, S. J. Kim, and D. Kim, "Profile effect on the feasibility of extinction-based localized surface plasmon resonance biosensors using metallic nanowires," Appl. Opt. **45**, 3382–3389 (2006).
15. D. Kim, "Effect of resonant localized plasmon coupling on the sensitivity enhancement of nanowire-based surface plasmon resonance biosensors," J. Opt. Soc. Am. A **23**,

2307–2314 (2006).
16. T. R. Michel, M. E. Knotts, and K. A. O'Donnell, "Scattering by plasmon polaritons on a rough surface with a periodic component," J. Opt. Soc. Am. A **12**, 548–559 (1995).
17. M. G. Moharam and T. K. Gaylord, "Diffraction analysis of dielectric surface-relief gratings," J. Opt. Soc. Am. **72**, 1385–1392 (1982).
18. M. G. Moharam and T. K. Gaylord, "Rigorous coupled-wave analysis of metallic surface-relief gratings," J. Opt. Soc. Am. A **3**, 1780–1787 (1986).
19. J. Lermé, "Introduction of quantum finite-size effects in the Mie's theory for a multilayered metal sphere in the dipolar approximation: application to free and matrix-embedded noble metal clusters," Eur. Phys. J. D **10**, 265–277 (2000).
20. E. Moreno, D. Erni, C. Hafner, and R. Vahldieck, "Multiple multipole method with automatic multipole setting applied to the simulation of surface plasmons in metallic nanostructures," J. Opt. Soc. Am. A **19**, 101–111 (2002).
21. K. M. Byun, D. Kim, and S. J. Kim, "Investigation of the sensitivity enhancement of nanoparticle-based surface plasmon resonance biosensors using rigorous coupled-wave analysis," in *Plasmonics in Biology and Medicine II*, T. Vo-Dinh, J. R. Lakowicz, and Z. K. Gryczynski, eds., Proc. SPIE 5703, 61–70 (2005).
22. J. Cesario, R. Quidant, G. Badenes, and S. Enoch, "Electromagnetic coupling between a metal nanoparticle grating and a metallic surface," Opt. Lett. **30**, 3404–3406 (2005).
23. E. D. Palik, *Handbook of Optical Constants of Solids* (Academic, 1985).
24. A. A. Maradudin and W. Zierau, "Effects of surface roughness on the surface-polariton dispersion relation," Phys. Rev. B **14**, 484–499 (1976).
25. T. S. Rahman and A. A. Maradudin, "Surface-plasmon dispersion relation in the presence of surface roughness," Phys. Rev. B **21**, 2137–2143 (1980).
26. C. L. Haynes, A. D. McFarland, L. Zhao, R. P. Van Duyne, G. C. Schatz, L. Gunnarsson, J. Prikulis, B. Kasemo, and M. Käll, "Nanoparticle optics: the importance of radiative dipole coupling in two-dimensional nanoparticle arrays," J. Phys. Chem. B **107**, 7337–7342 (2003).
27. S. Enoch, R. Quidant, and G. Badenes, "Optical sensing based on plasmon coupling in nanoparticle arrays," Opt. Express **12**, 3422–3427 (2004).
28. J. P. Kottmann and O. J. F. Martin, "Retardation-induced plasmon resonances in coupled nanoparticles," Opt. Lett. **26**, 1096–1098 (2001).